Semiconductor Photocatalysis.[1] ZnS-Nanocrystallite-Catalyzed Photooxidation of Organic Compounds

Shozo Yanagida,* Hiroshi Kawakami, Yoshihide Midori, Hirotoshi Kizumoto, Chongjin Pac, and Yuji Wada

Chemical Process Engineering, Faculty of Engineering, Osaka University, Suita, Osaka 565

(Received May 31, 1994)

Freshly prepared ZnS (nano-ZnS) suspensions catalyze photooxidation of organic substrates under band-gap irradiation with water as a good electron acceptor, while H_2 evolves concomitantly. The organic substrates with hetero atoms or carbon–carbon double bonds (π-bonds), such as triethylamine (TEA), diethylamine (DEA), methanol, ethanol, cyclopentene, cyclohexene, 2-methylfuran, toluene, and ethylbenzene, undergo effective one-hole oxidation. This leads to efficient carbon–carbon bond forming reactions between cumulatively formed radicals at the α-carbon adjacent to the hetero atom or the π-bond. The photooxidation in the presence of a larger quantity of water results in successive oxidation of the intermediary α-carbon radicals, giving the two-hole oxidation products, e.g., DEA and acetaldehyde from TEA, and formaldehyde from methanol. The formation of the intermediary α-carbon radical has been clarified by ESR analysis using 2-propanol as an organic substrate. Semi-empirical molecular orbital calculations suggest that the nano-ZnS-catalyzed photooxidation should be predictable from energetics in the formation of the α-carbon radicals through one-hole oxidation and deprotonation, and from change in the bond order of αC–H bond of the α-carbon cation radicals.

A series of our studies on ZnS photocatalysis has elucidated that the aqueous ZnS suspension prepared at ambient temperature from zinc sulfate and sodium sulfide consists of ZnS nanocrystallites and their loose aggregates (nano-ZnS). Such a suspension displays efficient photoredox reactions under irradiation ($\lambda > 290$ nm) of aqueous solution of organic substrates. The reduction of water by the conduction band electrons generates H_2. One-hole oxidation of cyclic ethers leads to the α-carbon–carbon bond formation through coupling of the intermediary α-carbon radicals.[2] Further, while defect-rich ZnS prepared in methanol catalyzes the cis–trans photoisomerization of some alkenes,[3] defect-free ZnS nanocrystallites (cubic) prepared under cooling in water photocatalyze the efficient reduction of carbonyl compounds[4,5] or of carbon dioxide (CO_2)[6] to the respective alcohols and formic acid, with concomitant photooxidation of appropriate sacrificial electron donors in the system. Elimination of surface defects which may be attributable to sulfur vacancies should be requisite for elongation of life time of conduction-band electrons which play an important role in the effective reduction of carbonyl compounds and CO_2. Contrary to these findings, we have noticed that some electrons trapped at shallow surface states of nano-ZnS contribute to H_2 evolution to an appreciable extent.

The intrinsic energy structure of nano-ZnS suggests that the conduction-band electrons have high potential for reduction but the valence-band holes have only moderate potential for oxidation.[5] The freshly prepared nano-ZnS suspension, however, showed an attractive photocatalysis for oxidation of some organic substrates, which was worth investigating because of mechanistic and synthetic interest. For example, methanol whose oxidation potential is 3.0 V vs. SCE, was oxidized to give ethylene glycol and/or formaldehyde in the nano-ZnS-catalyzed photoredox reaction of aqueous methanol.[7] Further, triethylamine (TEA) as well as some cyclic ethers underwent efficient one-hole oxidation, leading to effective coupling reactions of the intermediary α-carbon radical.[2] Such efficient and enhanced oxidizing power should be ascribed to the efficient oxidative quenching of the excited electron by water and the size quantization effect which should operate in the aqueous nano-ZnS system.

This work has been undertaken to clarify the scope and limitation of the one-hole oxidation in the photocatalysis with aqueous nano-ZnS suspensions. The nano-ZnS-catalyzed photolysis has been extended to aliphatic amines, alcohols, alkenes, and benzilic compounds. Here we also report mechanistic details of the efficient one-hole oxidation of organic molecules and their photo-oxidative carbon–carbon bond-making reactions through MO calculations.

Results and Discussion

Photolysis of Aliphatic Amines. Nano-ZnS-catalyzed photolysis of aqueous solutions of some nitrogen-containing organic compounds was undertaken. The H_2 evolution was monitored as a measure of the photooxidation activity, because it should correlate to the oxidation of the substrates in the photocatalysis as explained in Scheme 1. In Table 1 are summarized quantities of H_2 and the turnover numbers after 4 h irradiation. Aliphatic amines such as TEA and diethylamine (DEA), and *N*-methylpyrrolidine (NMP) were found to be readily oxidized, leading to effective H_2 evolution with large turnover numbers, while nitriles and amides were almost inert during the photolysis. The slight evolution of H_2 in the latter cases may be due to photo-degradation of the ZnS nanocrystallites themselves. As already reported,[8] the decreased H_2 evolution in the case of ethylamine can be explained as due to the competitive formation of DEA by the photoreduction of *N*-ethylideneethylamine (the Schiff base) which is readily formed by condensation of the amine and acetaldehyde produced by the preceded photooxidation of ethylamine.

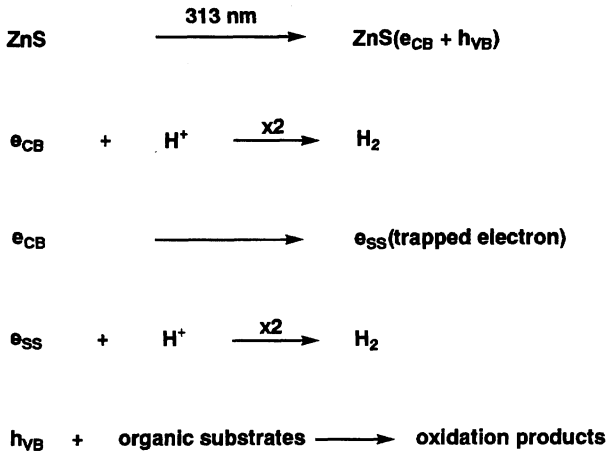

Scheme 1.

Table 1. Nano-ZnS-Catalyzed H_2 Evolution in Photolysis of Nitrogen-Containing Organic Compounds[a]

Substrate	H_2 evolved[b] mmol	Turnover number[c]
Triethylamine (TEA)	0.82	5.47
Diethylamine (DEA)	0.80	5.33
Ethylamine	0.16	1.07
Triethanolamine	0.22	1.47
N-Methylpyrrolidine	0.82	5.47
N-Methylpiperidine	0.32	2.13
N-Methylmorpholine	0.33	2.20
Acetonitrile	0.04[d]	0.20
Propiononitrile	0.02[e]	0.14
Acetamide	0.03[f]	0.20
Propionamide	0.03[f]	0.20

a) Method B: Organic compound 4 mL, nano-ZnS 0.15 mmol, water 6 mL, λ>290 nm. b) After 4 h irradiation. c) Determined by dividing the quantity of the evolved H_2 by the quantity of ZnS (diatomic). d) Nano-ZnS (0.20 mmol) and borate buffer solution (8 mL) instead of water were used. e) Borate buffer solution (6 mL) was used instead of pure water. f) Organic compound (1 g) and borate buffer solution (10 mL) were used.

To clarify the photooxidation products from TEA and DEA, large-scale photolysis (method c)[2] was undertaken under the conditions comparable to those for the small scale ones. In a large-scale photolysis of an aqueous solution of TEA (1:1 (v/v)) under cooling with ice and water, 2,3-bis(diethylamino)butane (**1**) and *threo*-3-(diethylamino)butane-2-ol (**2**) were isolated and identified as oxidation products (see Scheme 2).[7] Figure 1 shows time–conversion plots of their formation and H_2 evolution. After 5 h irradiation, acetaldehyde was added to the reaction mixture by assuming the participation of acetaldehyde formed by hydrolysis of the two-hole oxidation product of TEA, i.e., *N*-ethylidenediethylammonium salt (**3**), in the photolysis. As expected, the continued photolysis led to an increase of the formation of the amino alcohol **2**, followed by slight decreases in the formation of the dimer **1** and H_2. The decrease of H_2 evolution must be due to the consumption of the photoformed electrons by the reduction of acetaldehyde. These experimental results indicate that the one-electron reduction of acetaldehyde should participate in the formation of the amino alcohol **2**.

When the photocatalysis of TEA was carried out after diluting with a large quantity of water, diethylamine was produced almost in proportion to H_2 evolution as shown in Fig. 1b. These observations suggest that the coupling reactions to the dimer **1** and the amino alcohol **2** should require the effective accumulation of the α-carbon radicals from TEA. In the photolysis of the highly diluted aqueous TEA system, the sequential two-hole oxidation of TEA should prevail, giving DEA and acetaldehyde through hydrolysis of the ammonium salt **3**.

As for the photolysis of DEA under the comparable conditions, stereoisomeric mixtures of 1,3-diethyl-2,4,5-trimethylimidazolidine (**5**) (*d,l* and *meso*) were isolated as oxidation products. Figure 2a shows time-conversion plots of the formation of H_2 and the cyclic dimer **5**. Since the coupling product, 2,3-bis-(ethylamino)butane (**4**), was conceived as a precursor of the cyclic dimer **5**, GLC analyses were conducted after adding excess acetaldehyde (10—25 mmol) into the photolysate. The increased yields of the cyclic dimer **5** were confirmed, as shown by the dotted line in Fig. 2a. The difference in quantity between the dotted and solid lines should correspond to the formation of dimer **4**, since dimer **4** readily reacts with acetaldehyde, giving the cyclic dimer **5**. Interestingly, the photoredox reaction of a highly concentrated aqueous DEA system (Fig. 2a) gave an acceptable electron balance, i.e., the formation of the

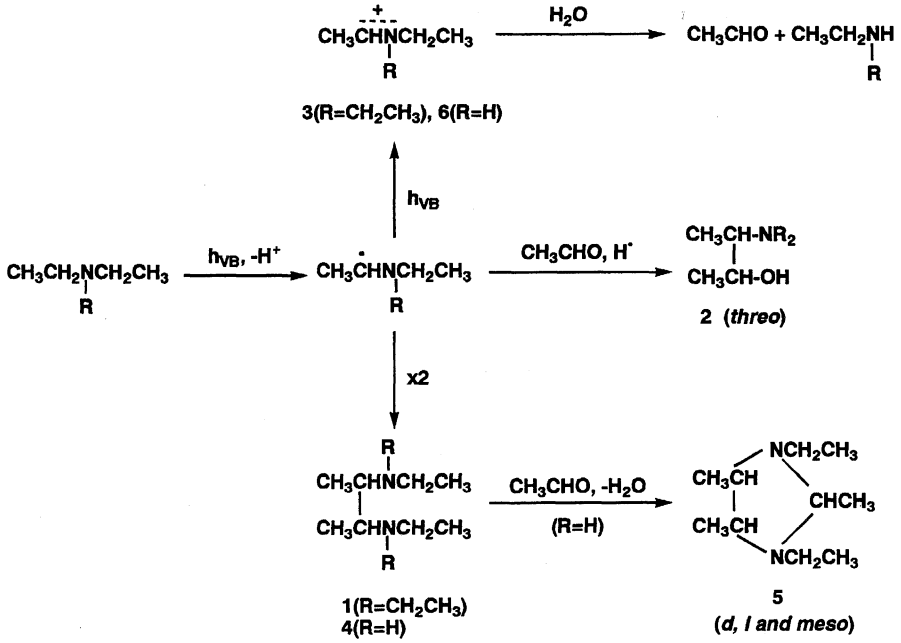

Scheme 2.

cyclic dimer **5** corresponded to the formation of two molecules of H_2, and the formation of the dimer **4** to the formation of one molecule of H_2. In fact, side reaction products, such as amino alcohols like **2**, could not be detected.

Photolysis of DEA in high dilution with water also resulted in exclusive formation of ethylamine with efficient H_2 evolution (Fig. 2b). The two-hole oxidation of DEA to *N*-ethylideneethylammonium salt **6** as a precursor of ethylamine should prevail in the diluted system. In the photolysis of the highly diluted TEA system (Fig. 1b), ethylamine was detected after the prolonged irradiation. The observation can be explained as due to the two-hole oxidation of the initially produced DEA.

Based on the above-mentioned observations, reaction paths in the photolysis of TEA and DEA, can be depicted as shown in Scheme 2.

Photolysis of Aliphatic Alcohols. As shown in Fig. 3, the photolysis of aqueous methanol (3 : 1 (H_2O) v/v) with nano-ZnS led to the formation of both formaldehyde and ethylene glycol (EG) with efficient H_2 evolution. EG was found to form after an induction period, while formaldehyde started to form from the initial stage. Although the two products can be explained to be formed through hydroxylmethyl radical **7** (see Scheme 3), the induction period observed for the formation of EG implies another mechanism involving the formation of formaldehyde as an intermediate.

After 8 h photolysis of methanol with less H_2O (4 : 1 (H_2O) v/v) examined under comparable conditions (Fig. 4), formaldehyde (15 mmol) was added to the photolysate, and the formation of H_2 and EG was monitored as shown in Fig. 4. The rate of H_2 evolution was almost unchanged, but the rate of the EG formation became 2.5 times as fast as the original rate. This observation leads to a mechanism involving an addition of hydroxylmethyl radical **7** to formaldehyde followed by hydrogen abstraction (Scheme 4). Such a mechanism would explain the induction period observed at the initial stage; the enhancement of EG formation observed by addition of formaldehyde without affecting H_2 formation would be explained. The result that addition of formaldehyde has no effect on H_2 evolution eliminates

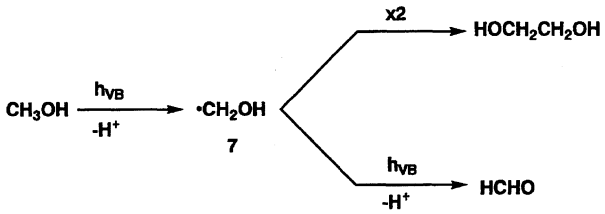

Scheme 3.

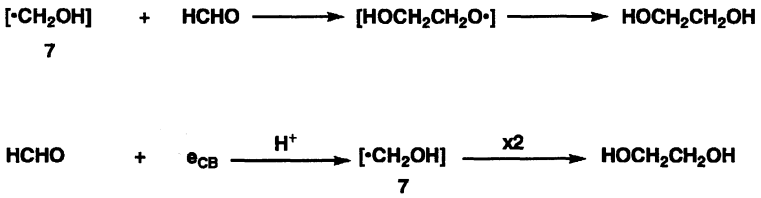

Scheme 4.

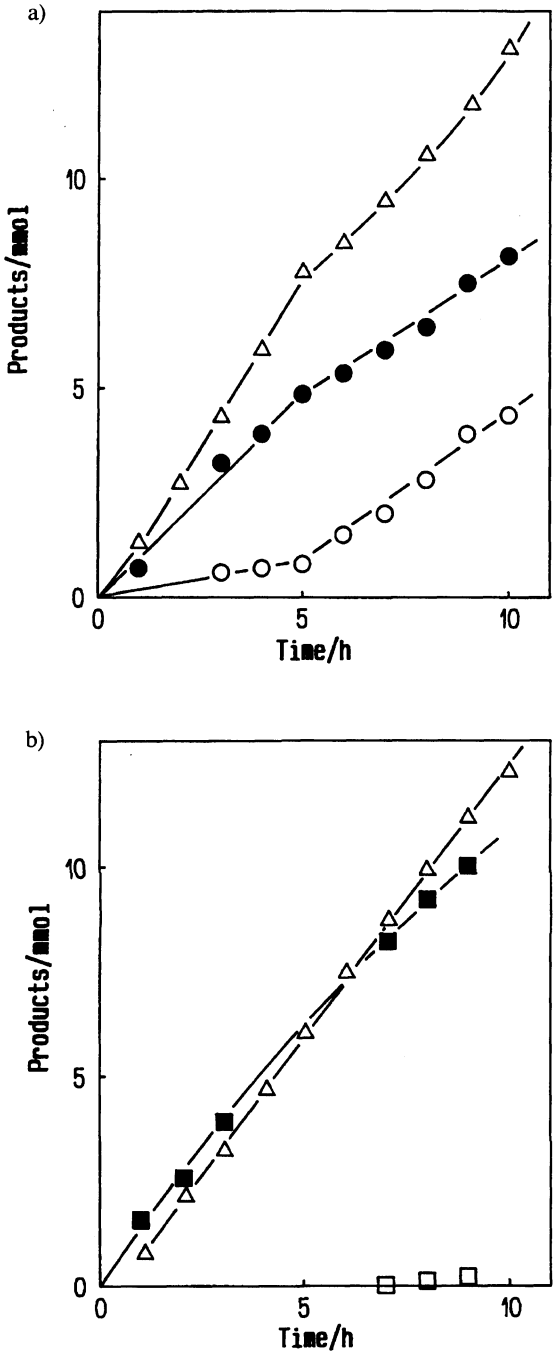

Fig. 1. Nano-ZnS-catalyzed photolysis of triethylamine (TEA). a) TEA 200 mL and water 200 mL, ZnS 5 mmol, Hg arc lamp 100 W. (●), 2,3-bis(diethylamino)butane (**1**); (○), *threo*-3-diethylamino-2-butanol (**2**); (△), H_2. b) TEA, 10 mL, water 400 mL, ZnS 5 mmol. (the diluted TEA). (■), DEA; (□), ethylamine; (△), H_2.

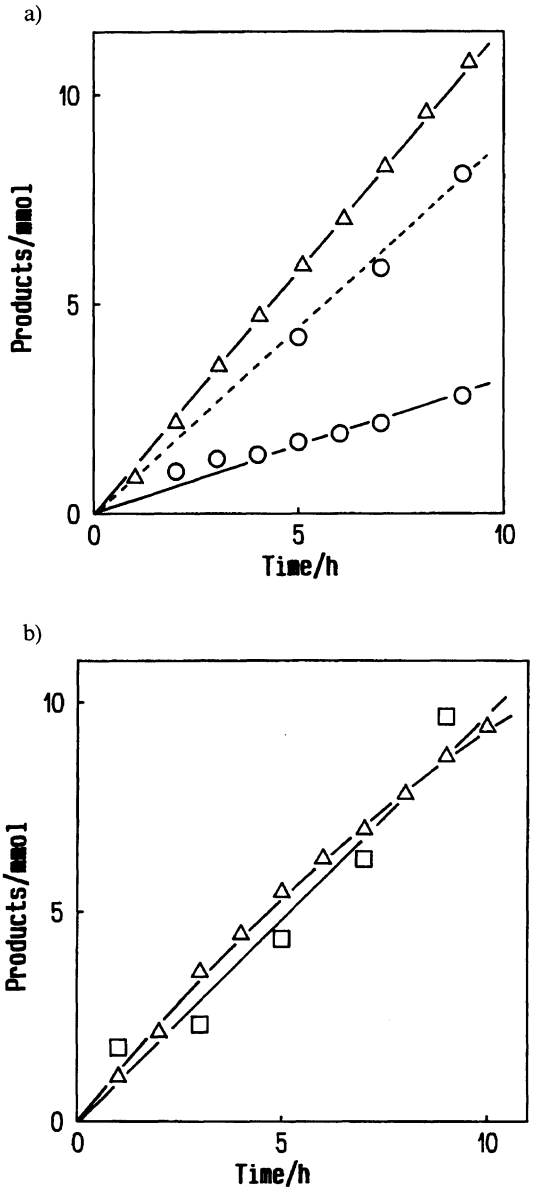

Fig. 2. Nano-ZnS-catalyzed photolysis of diethylamine (DEA). a) DEA 200 mL, water 200 mL, ZnS 5 mmol, Hg arc lamp 100 W. (○), 1,3-diethyl-2,4,5-trimethylimidazolidine (**5**); (△), H_2. b) DEA 10 mL, water 400 mL, ZnS 5 mmol. (the diluted DEA). (□), ethylamine; (△), H_2.

participation of the radical **7** formed by reduction of formaldehyde in the formation of EG.

The nano-ZnS-catalyzed photolysis was extended to some other alcohols; the results are summarized in Table 2. The α-carbon–carbon bond formation reaction could be confirmed for ethanol, 2-propanol, and benzyl alcohol in fair to good yields. It is worth noting that 2-methyl-2-propanol, which has no α-hydrogen, gave a trace amount of 2,5-dimethyl-2,5-hexanediol. This result is due to the one-hole oxidation of the methyl groups of 2-methyl-2-propanol, leading to the coupling of the resulting β-carbon radical.

Photolysis of Alkenes and Benzylic Compounds with Water. Figures 5 and 6 show H_2 evolution in the nano-ZnS catalyzed photolysis of either alkenes or benzylic compounds in the presence of water. These organic substrates are sparingly insoluble in water, giving heterogeneous reaction systems consisting

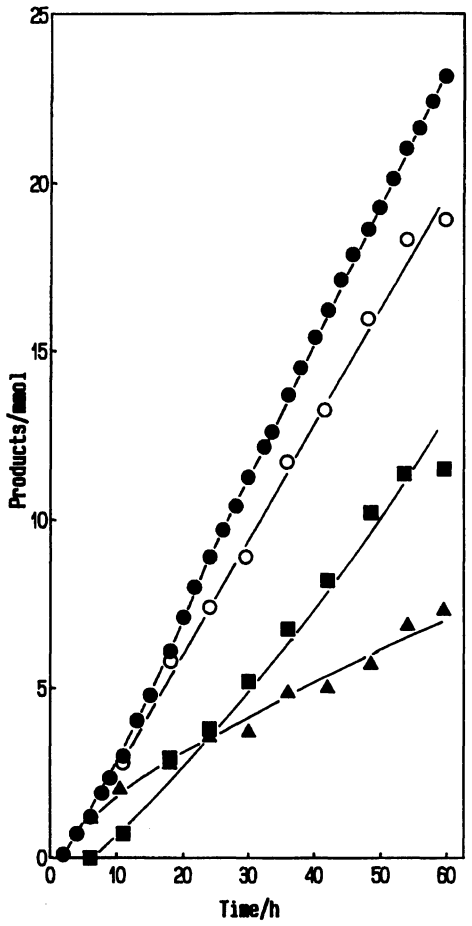

Fig. 3. Nano-ZnS-catalyzed photolysis of aqueous methanol. (methanol 300 mL, water 100 mL, ZnS 2 mmol, Hg arc lamp 100 W). (●), H_2; (▲), formaldehyde; (■), EG; (○), total of formaldehyde and EG.

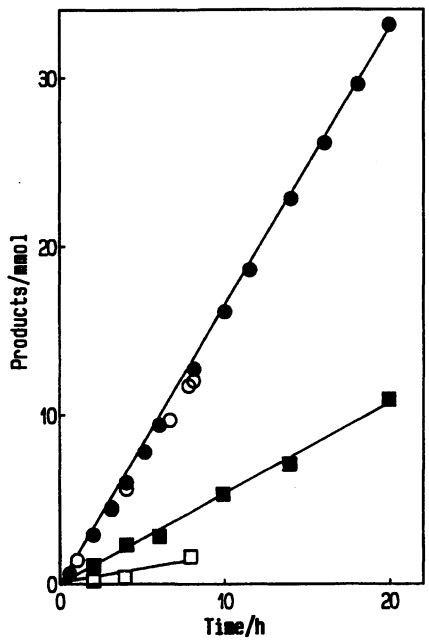

Fig. 4. Effect of the addition of formaldehyde on nano-ZnS-catalyzed photolysis of aqueous methanol (methanol 400 mL, water 100 mL, ZnS 5 mmol, Hg arc lamp 300 W). (●), H_2 evolved after the addition of formaldehyde (15 mL); (○), H_2 evolved under the initial conditions (before the addition of formaldehyde); (■), EG formed after the addition of formaldehyde; (□), EG formed under the initial conditions (before the addition of formaldehyde).

of water, nano-ZnS and the dispersed substrate. Previously we reported that some alkenes undergo ZnS-catalyzed photoisomerization in methanol followed by gradual photooxidation.[3] It has now been found that some alkenes and benzylic compounds are readily photooxidized in the aqueous nano-ZnS system, and effective H_2 evolution could be observed in the presence of cyclopentene, cyclohexene, 2-methylfuran, 2,5-dimethylthiophene, 2,5-dimethylfuran, ethylbenzene, and tol-

Table 2. Nano-ZnS-Catalyzed Photolysis of Alcohols[a)]

Alcohol	H_2	Oxidation products	Quantum yield
	mmol	mmol	$(\Phi_{1/2H_2})^{b)}$
Methanol	0.321	Formaldehyde (0.154) Ethylene glycol (0.124)	0.13
Ethanol	0.521	Acetaldehyde 2,3-Butanediol (0.188)	0.14
2-Propanol	0.447	Acetone 2,3-Dimethyl-2,3-butanediol (0.056)	0.24
2-Methyl-2-propanol	0.049	2,5-Dimethyl-2,5-hexanediol (trace)	—
Benzyl alcohol	0.553	Benzaldehyde 1,2-Diphenylethanediol	—

a) Method A: alcohol 10.8 mL, water 1.2 mL, nano-ZnS 0.05 mmol, $\lambda > 290$ nm, 4 h.
b) Apparent quantum yields were determined by method C: alcohol 1 mL, water 3 mL, ZnS 0.02 mmol, $\lambda = 313$ nm, $I = 4.2 \times 10^{15}$ photon/s, 10—20 h irradiation.

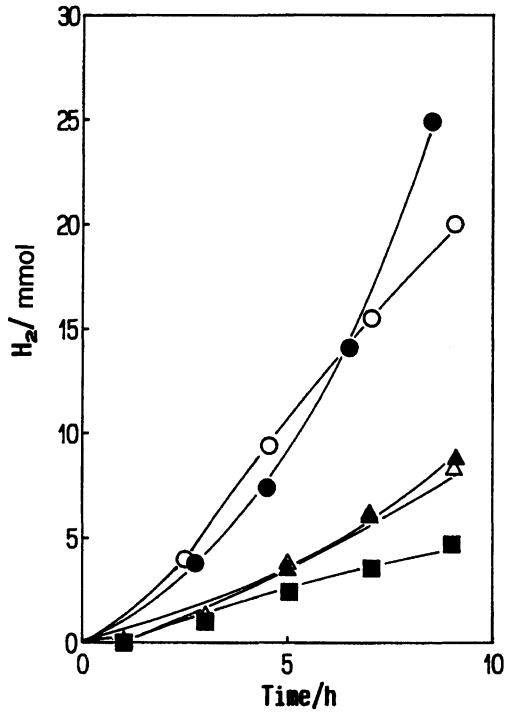

Fig. 5. Nano-ZnS-catalyzed H_2 evolution in the photolysis of aqueous suspension of alkenes. (●), in photolysis of cyclopentene; (○), cyclohexene; (▲), 2-pentene (*cis* and *trans*); (△), 2-hexene (*cis* and *trans*); (■), *cis*-2-octene.

uene. *t*-Buthylbenzene worked as an electron donor for H_2 evolution, as was confirmed for 2-methyl-2-propanol, implying the slow oxidation of molecules with *t*-butyl group in the nano-ZnS catalyzed photolysis.

Some photolyses were carried out on a large scale; their oxidation products were analyzed as summarized in Table 3. Cyclopentene, cyclohexene, and 2-methylfuran afforded the α-carbon–carbon bond formation products in fair yields. When the recovered ZnS was extracted with a Soxhlet using petroleum ether, oligomeric products ranging from trimer to hexamer were obtained in every case. Further, FT-IR spectra of each isolated nano-ZnS powder showed absorption around 2800—2900 cm^{-1}, suggesting that successive oxidation of products should occur through strong adsorption onto nano-ZnS, contributing to the slight increase of H_2 evolution and the formation of oligomeric products under the prolonged irradiation.

Toluene and ethylbenzene also gave coupling products with many side-reaction products, including some unidentified ones. The mass spectral analysis of the oligomeric products from toluene indicated the formation of dibenzyl sulfide and dibenzyl disulfide. An electrophilic benzyl cation should be produced by two-hole oxidation of toluene, resulting in the reactions with nucleophilic sulfide and disulfide ions in the reaction system. The blackening of nano-ZnS was often observed during the photolysis; this is explained as due to the

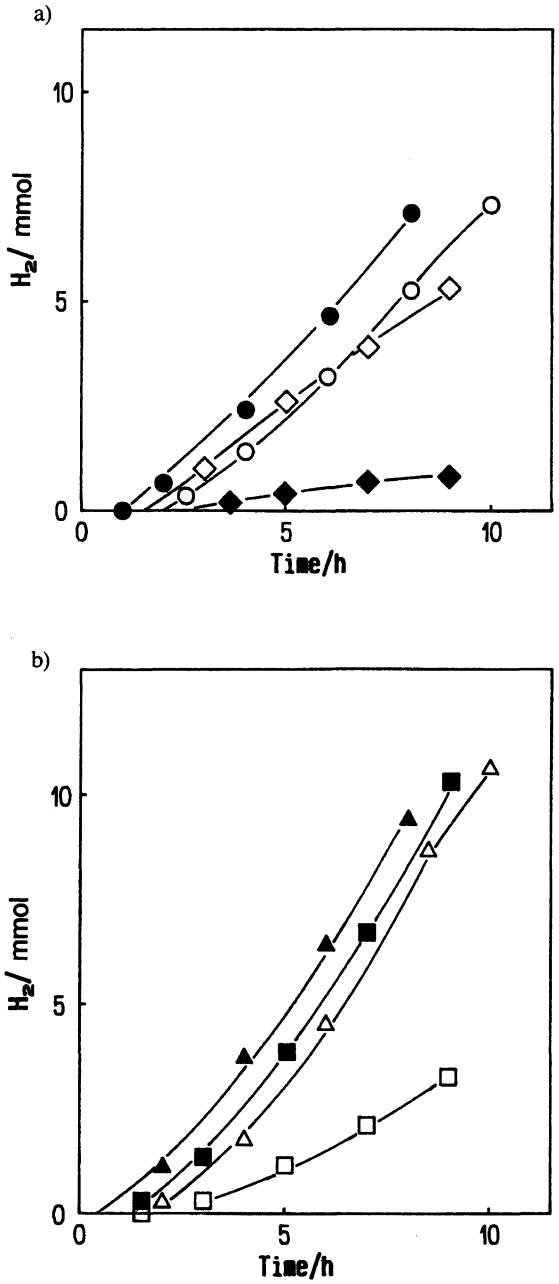

Fig. 6. Nano-ZnS-catalyzed H_2 evolution in the photolysis of aqueous suspension of benzylic compounds. a) (●), in photolysis of ethylbenzene; (○), toluene; (◇), cumene. (◆), *t*-butylbenzene. b) (▲), in the photolysis of 2-methylfuran; (△), 2,5-dimethylfuran; (■), 2,5-dimethylthiophene; (□), 2,5-dimethylpyrrole.

formation of metallic Zn in the lattice. Oily products probably hinder electron-accepting water from adsorbing on the ZnS surface.

Quantum Efficiency of Nano-ZnS Catalyzed Photoredox Reactions. Action spectrum was obtained by monitoring quantum yields of H_2 evolution in the nano-ZnS-catalyzed photolysis of DEA (Fig. 7). The high quantum efficiency for H_2 evolution ($\Phi_{1/2H_2}$=0.82)

Table 3. Nano-ZnS-Catalyzed Photolysis of Alkenes and Benzylic Compounds[a)]

Substrate	Reaction time/h	H_2 mmol	Oxidation products[b)] mmol
Cyclopentene	9	13.2	Bi-3-cyclopenten-1-yl (dl, *meso*)(1.8), Oligomer[c)] (4.2[d)]), 2-Cyclopenten-1-one (trace)
Cyclohexene	13	10.8	Bi-3-cyclohexen-1-yl (*dl*, *meso*) (0.9), Oligomer[c)] (9.5[d)]), 2-Cyclohexen-1-one (trace)
2-Methylfuran	8	9.5	1,2-Di(2-furyl)ethane (*dl*, *meso*) (2.7), Oligomer(5.8), 2-Furaldehyde (trace)
Toluene	12	3.4	Bibenzyl (0.4), Benzaldehyde (trace), Benzoic acid (trace), Stilbene (trace) Oligomer (dibenzyl sulfide, dibenzyl disulfide) (136 mg)
Ethylbenzene	12	7.3	2,3-Diphenylbutane (*dl*, *meso*) (1.6), 2,3-Diphenyl-2-butanol (*threo*, *erythro*) (2.0), 2,3-Diphenyl-2,3-butanediol(*dl*, *meso*) (0.4), Acetophenone (trace), Oligomer

a) Method A: substrates 10 mL, water 490 mL, ZnS 5 mmol, pH 7. b) GLC yield. c) Oligomers ranging from trimer to hexamer were estimated from analysis of mass spectra. d) Values are based on monomer unit.

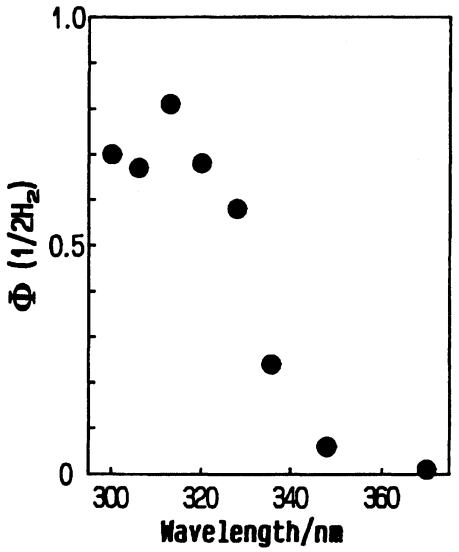

Fig. 7. Action spectrum of nano-ZnS-catalyzed H_2 evolution in the photolysis of aqueous DEA.

was observed at 310 nm. The spectrum was quite comparable with that obtained for the nano-ZnS-catalyzed photoreduction of 2-butanone to 2-butanol.[5)] Further, the set-up in the action spectrum was very close to that of the absorption spectrum of the nano-ZnS suspension.

In Table 4 are summarized apparent quantum yields for H_2 evolution obtained in the photolysis of some organic substrates. When compared with their oxidation potentials and/or ionization potentials (IP), the quantum efficiency has a rough tendency to increase with ease of oxidation of substrates, except for cyclic alkenes.

It is worth noting that methanol and ethanol, whose oxidation potentials are around 3.0 V vs. SCE, were oxidized with slow rates. As reported,[5)] nano-ZnS has a distribution in particle size. When some much smaller particles are excited, they might exhibit outstanding oxidation power. Careful reexamination of the TEM picture of the nano-ZnS suspensions well explains the presence of nano-scale ZnS particles whose sizes range from less than 3 nm to 5 nm in diameter. Further, the nano-ZnS showed the band gap emission with two peaks at 323 and 334 nm. The enhanced oxidizing power in the nano-ZnS-catalyzed photolysis would be explained as due to the size quantization effect based on the presence of molecular-scale ZnS particles.[10)]

Detection of an α-Carbon Radical in the Nano-ZnS Catalyzed Photolysis of Aqueous 2-Propanol. The α-carbon–carbon bond formation can be explained as a coupling reaction of the α-carbon radicals which are formed by one-hole oxidation and deprotonation of organic substrates on the UV-irradiated nano-ZnS. In order to detect an intermediary α-carbon radical in the photolysis, the photoformed species from 2-propanol was investigated by means of electron spin resonance spectrometry (ESR). The ESR measurement was conducted during the photolysis of 2-propanol with nano-ZnS under laser irradiation (309 nm). A gradual increase of temperature from liquid nitrogen boiling point to 183 K gave the ESR signals shown in Fig. 8. The *g*-value and the hyperfine structure support the structure of the α-carbon radical derived from 2-propanol. To the best of our knowledge, this is the first observation of a radical species formed in ZnS photocatalysis. 2,3-Dimethyl-2,3-butanediol in the photolysis of 2-propanol must be formed through the coupling

Table 4. Relationship between Quantum Efficiency ($\Phi_{1/2H_2}$) and Oxidation Potential or Ionization Potential of Substrates

Electron donor	$\Phi_{1/2H_2}$ [a]	Oxidation potential [b]	IP [c]
		$E^{1/2}$/V vs. SCE	eV
Methanol	0.04(0.13)[d]	3.06	10.84
Ethanol	0.04(0.14)[d]	2.94	10.49
1-Propanol	(0.22)[d]	2.89	10.10
2-Propanol	(0.24)[d]	2.83	10.15
2-Pentene	0.11	3.10[e]	9.11 (cis) 9.06 (trans)
2-Hexene	0.09	3.10[f]	
Cyclopentene	0.43	—	9.01
Cyclohexene	0.21	2.17	8.72
Toluene	0.08	1.98	8.82
Ethylbenzene	0.10	1.90[g]	8.76
TEA	0.20	0.94	7.50
DEA	0.30	0.764	8.01

a) Method C: substrate 0.2 mL, water 3 mL, nano-ZnS 25 mmol, $\lambda=313$ nm, $I=4.2\times10^{15}$ photon/s. b) Determined in acetonitrile and corrected in SCE unit. See Ref. 13 c) See Ref. 14. d) The quantity of the substrate was increased to 1 mL. e) The value for 1-pentene. f) The value for 1-hexene. g) Determined in methanol.

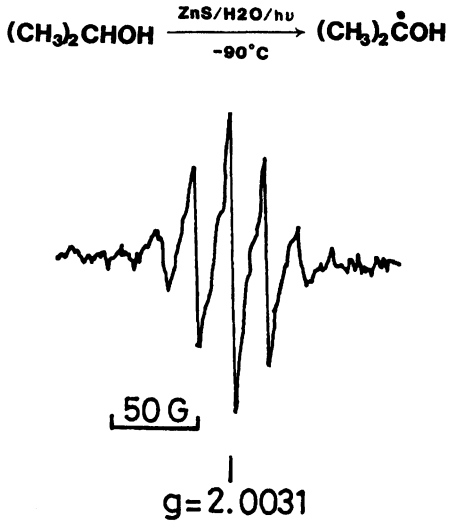

Fig. 8. Electron spin resonance spectrum of the radical detected in the nano-ZnS-catalyzed photolysis of 2-propanol.

of the α-carbon radical observed in the ESR spectrum. The same coupling mechanism should operate for the other substrates examined in the present work.

Molecular Orbital Calculations of Possible Intermediates in the Photolysis. Free carbon radicals adjacent to lone pairs of hetero atoms like nitrogen and oxygen, or to π bonds like carbon–carbon double bond, are stabilized by conjugative delocalization of the unpaired electron.[12] In order to estimate the ease of the formation of α-carbon radicals as intermediates of the coupling products in the present system, semi-empirical MO calculations were conducted for some alcohols, DEA, TEA, cyclopentene, cyclohexene, 2-methylfuran, and toluene. Heats of formation of the ground states were obtained for their energetically optimized structures; their cation radicals which are formed by one-hole oxidation and their α-carbon radicals which are formed through deprotonation from the cation radicals were also distinguished (Table 5).

The differences in the heat of formation between the ground states (neutral) (N) and the cation radicals (CR) (denoted as ΔH(CR–N) in Table 5) show the order of TEA<DEA<2-methylfuran<cyclohexene<toluene<cyclopentene<2-propanol<ethanol<methanol. This order coincides well with that of their oxidation potentials or that of the ionization potentials (IP) (Table 5). The excellent coincidence makes it reasonable to use the heat of formation calculated by MOPAC/PM3 for the mechanistic discussion of the photolysis. On the other hand, the feasibility of the formation of the α-carbon radicals will be in the order of 2-propanol>DEA>TEA>ethanol>cyclohexene>methanol>cyclopentene>2-methylfuran>toluene, as determined from the differences in heat of formation (ΔH(R–N)) between the α-carbon radicals and the ground states. The highest feasibility of the formation of the α-carbon radical of 2-propanol predicted here is justified by the ESR observation of the radical.

These data suggest that the MO calculations employed here are applicable to the estimation of the energetics, the geometry, and the electronic structures of intermediary species involved in the present one-hole photooxidation. Very effective H_2 evolution in the photolysis of TEA, DEA, cyclohexene, and cyclopentene can be explained by the energetics, i.e., the formation of the cation radicals (ΔH(CR–N)) and that of α-carbon radicals (ΔH(R–N)). The low efficiency observed for toluene should be attributed to the difficulty in the formation of the α-carbon radical predicted from the

Table 5. Semi-Empirical Molecular Orbital Calculation of Heat of Formation for Cation Radical and α-Carbon Radical from Substrate[a)]

Substrate	H(N)[b)]	H(CR)[c)]	H(R)[d)]	ΔH(CR–N)[e)]	ΔH(R–CR)[f)]	ΔH(R–N)[g)]
Methanol	−50.978	192.816	−23.480	243.794	−216.296	27.498
			−6.759[h)]		−199.575[h)]	44.219[h)]
Ethanol	−56.855	184.818	−33.666	241.673	−218.484	23.189
2-Propanol	−63.948	173.650	−44.484	237.598	−218.134	19.464
DEA	−23.252	166.441	2.335	186.693	−164.106	22.587
TEA	−25.747	154.994	−2.718	180.741	−157.712	23.029
Cyclohexene	−4.880	203.992	21.491	208.872	−182.501	26.371
Cyclopentene	3.019	212.857	30.853	209.838	−182.004	27.834
2-Methylfuran	−12.784	187.949	21.097	200.733	−166.852	33.881
Toluene	14.112	223.688	52.770	209.576	−170.918	38.658

a) Expressed in kcal mol^{-1}. b) Heat of formation of a neutral molecule. c) Heat of formation of a cation radical. d) Heat of formation of α-carbon radical. e) H(cation radical)−H(neutral). f) H(radical)−H(cation radical). g) H(radical)−H(neutral). h) Calculated as methoxyl radical instead of hydroxymethyl radical.

largest value of ΔH(R–N). In addition, the fact that formation of hydroxylmethyl radical is much easier than that of methoxyl radical is worth noting, since it well explains the effective coupling reaction of methanol on irradiated nano-ZnS. Furthermore, the energetics for the formation of the α-carbon radicals for alcohols has been found as favorable as those for TEA and DEA. This result supports the conclusion that photoredox reactions in the irradiated nano-ZnS system should be strongly influenced by the energetics, which correlates with the irreversible formation of the α-carbon radicals rather than with their ionization potentials.[5)]

The bond order of the ground states and the cation radicals was also calculated from the energetically optimized structures. The change in the bond order calculated for methanol, TEA, cyclohexene, cyclopentene, and toluene is demonstrated in Fig. 9. The large decrease in the bond order of αC–H bond in methanol cation radical supports the easy formation of hydroxylmethyl radical from the cation radical by deprotonation. A similar decrease in bond order was also obtained for TEA, cyclohexene, cyclopentene, and toluene. In particular, the large decrease in the bond order of αC–H bond in their cation radicals is in good agreement with the formation of the coupling compounds in the photocatalysis. This fact also implies that the cation radical of TEA should be so favorable for irreversible formation of the α-carbon radical by quick deprotonation that TEA can work as a good sacrificial electron donor for some photosensitized or photocatalyzed redox reactions. It should be emphasized that the energetics in the formation of the α-carbon radicals and the bond order in the intermediary cation radicals are good measures for the effective photooxidation on semiconductor particles.

Conclusion

The main conclusions to be drawn are as follows.

1) Freshly prepared ZnS nanocrystallites suspensions show powerful photocatalysis in photooxidation of some organic compounds, with concomitant reduction of water to H_2.

2) The organic substrates which may afford energetically favorable α-carbon radicals give their coupling products in the photooxidation with nano-ZnS.

3) The enhanced oxidizing power of nano-ZnS can be ascribed to the size quantization effect.

4) Accumulative formation of α-carbon radicals is decisive for the effective carbon–carbon bond formation reactions.

5) Semi-empirical MO calculation provides informative energetics and bond orders of cation radicals and free radicals as intermediates in the photooxidation.

The photocatalysis of semiconductor particles can be regarded as electrolysis by nano-sized electrodes dispersed in solution, i.e., by the conduction band as a cathode and the valence band as an anode. The photoredox reactions with semiconductor photocatalysts will be a fruitful research field as a novel method of photo-induced electro-organic synthesis.

Experimental

Materials. Sodium sulfide, zinc sulfate, commercially available ZnS (Nacalai), and other conventional chemicals were identical with those described in previous papers.[2—5)] Triethylamine (TEA) (Wako), diethylamine (DEA) (Wako), *N*-methylpyrrolidine (Tokyo Kasei), *N*-methylpiperidine (Aldrich), *N*-methylmorpholine (Aldrich), triethanolamine (Nacalai), acetonitrile (Nacalai), cyclopentene (Tokyo Kasei), cyclohexene (Wako), cyclooctene (Wako), ethylbenzene (Wako), 2-methylfuran (Nacalai), 2,5-dimethylfuran (Tokyo Kasei), 2,5-dimethylthiophene (Aldrich), 2-pentene (cis & trans) (Wako), and 2-hexene (cis & trans) (Nacalai) were purified by distillation before use. Benzyl alcohol (Wako), propionitrile (Nacalai), acetamide (Nacalai), and propionamide (Nacalai) were used as delivered.

Analyses. Product analysis was carried out by gas chromatography using a Shimadzu GC-7A apparatus equipped

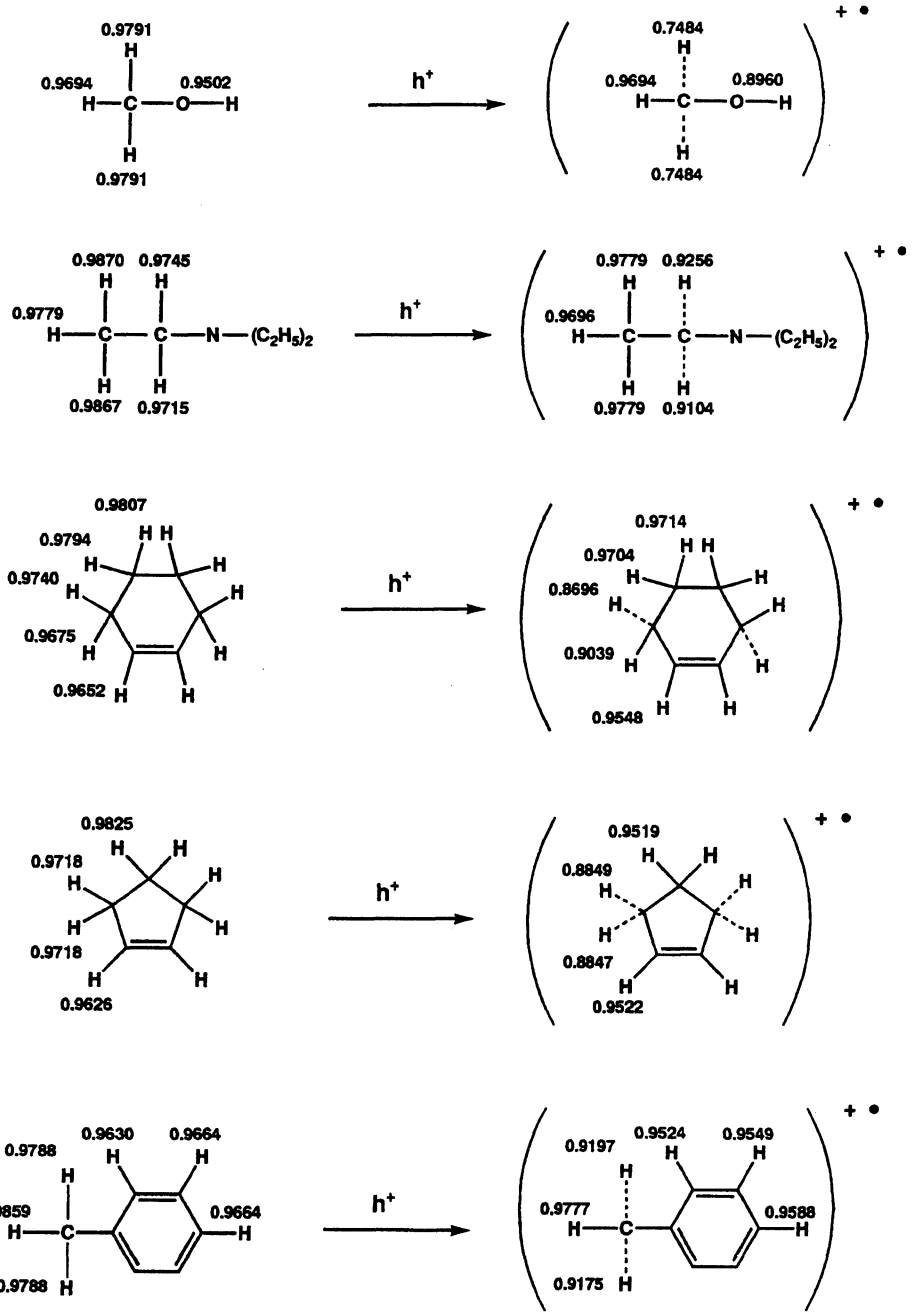

Fig. 9. Changes in the bond order calculated by the semi-empirical MO method for the ground states and the radical anions of the substrates. The numbers indicate the bond orders of the C–H bonds.

with flame ionization detectors. The following columns were used; Activated carbon 2 m (373 K) and Porapak Q 0.5 m for gas analysis, ASC-L 3 m for DEA and ethylamine, Ucon oil 550XLB 2 m for other amines, alcohols, aldehydes, and 1,2-di(2-furyl)ethane, Porapak Q 1 m for diols, Porapak T 2 m for formaldehyde, Silicon Gum SE-30 1 m for bi-3-cyclopenten-1-yl, bi-3-cyclohexen-1-yl, and bibenzyl. ^{1}H NMR, ^{13}C NMR, mass, IR, and UV spectra were obtained as mentioned in the previous paper.[2] The ESR signals were detected with a JEOL-FE3X ESR spectrometer under laser excitation (Lumonics TE-861M excimer laser; XeCl 308 nm, 20—30 mJ/pulse). Temperature was controlled with an Oxford ESR-900 continuous flow cryostat.

General Procedure of Nano-ZnS-Catalyzed Photolysis. Each nano-ZnS suspension was prepared at ambient temperature from aqueous zinc sulfate and sodium sulfide as reported in the previous paper.[2] The amount of nano-ZnS suspension was expressed in mol of diatomic ZnS unit. Three general methods A (small scale), B (medium scale), and C (large scale) were identical with those reported in the same paper.

Photolysis of TEA and Isolation of Oxidation Products. According to method C, a mixture of nano-ZnS (5 mmol), TEA (200 mL), and water (200 mL) was irradiated at 276 K for 10 h. H_2 (16.2 mmol) was evolved. The reaction mixture was extracted with diethyl ether and

the extract was distilled and condensed to 20 mL. The residue was dried with anhydrous Na_2SO_4; 2,3-bis(diethylamino)butane (**1**) and *threo*-3-diethylamino-2-butanol (**2**) were isolated by fractional distillation under reduced pressure. The dimer **1**: yield (GLC, 11.5 mmol); bp 70—75 °C/4.5 Torr (1 Torr=133.322 Pa), ^{1}H NMR (60 MHz, d_6-acetone) δ=1.8—3.00 (m, 10H) and 0.7—1.28 (m, 18H); MS *m/z* (rel intensity) 200 (M^+), 144 (51), 128 (51), 100 (100), 84 (33), 72 (82). Anal. Found: C, 71.89; H, 14.18; N, 13.89%. Calcd for $C_{12}H_{28}N_2$: C, 71.93; H, 14.09; N, 13.98%. GLC analysis (Ucon oil) showed two peaks of equal areas due to the *dl* and *meso* forms. The amino alcohol **2**: yield (GLC, 2.7 mmol); bp 46—48 °C/7.5 Torr, ^{1}H NMR (60 MHz, d_6-acetone) δ=0.82—1.28 (m, 12H), 2.08—2.95 (m, 5H), 3.08—3.52 (m, H, OH). The coupling constant between CHOH and $CH_3CHN(Et)_2$ was 8—9 Hz, suggesting the threo form of **2**; MS *m/z* (rel intensity) 145 (M^+; 2), 144 (5), 130 (27), 100 (87), 84 (13), 72 (100). Found: C, 65.89; H, 13.28; N, 9.75%. Calcd for $C_7H_{18}NO$: C, 66.16; H, 13.19; N, 9.64%.

Photolysis of DEA and Isolation of Oxidation Products. According to method C, a mixture of nano-ZnS suspension (5 mmol), DEA (200 mL), and water (200 mL) were irradiated at 276 K for 10 h, leading to H_2 (12.6 mmol) evolution. The similar treatment of the reaction mixture gave a fraction of products, bp 47 °C/7.5 Torr. Column chromatography using basic alumina and 1:20 mixture of methanol and petroleum ether as eluent gave 1,3-diethyl-2,4,5-trimethylimidazolidine (**5**) as an oily product. The product **5** was further purified by distillation and analyzed as a mixture of three stereo isomers. GPC analysis (Ucon oil) at column temperature, 403 K, showed three peaks of 1:2:1 areas due to the cyclization of the *dl* and *meso* forms of 2,3-bis(ethylamino)butane (**4**). ^{1}H NMR (60 MHz, d_6-acetone) δ=0.62—1.20 (m, 15H), 2.12—2.85 (m, 6H), 3.04 (q, H), 3.70 (q, H); ^{13}C NMR (15 MHz, d_6-acetone) δ=14.2, 14.9, 16.2, 18.5, 20.5 (CH_3), which support the above-mentioned structures of three isomers. 40.4, 49.0 (CH_2), 62.0, 66.8 (NCCH$_3$), 77.3 (NCHN). MS *m/z* (rel intensity) 170 (M^+), 155 (2), 145 (1), 144 (1), 100 (1), 73 (17), 72 (100). Anal. Found: C, 70.24; H, 13.13; N, 16.34%. Calcd for $C_{10}H_{22}N_2$: C, 70.53; H, 13.02; N, 16.45%. The water phase of the reaction mixture was condensed by azeotropic distillation using benzene, giving a benzene solution of **4**. The distillate, 37—40 °C/5 Torr was found to be a mixture of **4** and **5**. Chromatography over basic alumina with diethyl ether and with methanol gave **4** as an apparently homogeneous oil of greater than 90% purity (TLC). ^{1}H NMR δ=0.83—1.33 (m, 12H), 2.26—2.97 (m, 6H). MS *m/z* (rel intensity) 143 (M^+-1), 142 (2), 128 (5), 127 (4), 100 (2), 72 (100). The reaction of the dimer **4** with acetaldehyde was confirmed to give the cyclic dimer **5** by GPC.

Photolysis of Cyclopentene and Characterization of Products. According to method C, a mixture of nano-ZnS suspension (5 mmol), cyclopentene (10 mL), and water (490 mL) was irradiated at room temperature for 9 h. H_2 evolution (13.2 mmol) was observed. It is interesting to note that the ZnS coagulated and existed at the oily phase. The reaction mixture was extracted three times with dichloromethane using a centrifuge. After evaporation of the solvent, chromatography over basic alumina (4.5 wt% water) with petroleum ether, followed by Kugelrohr distillation gave bi-3-cyclopenten-1-yl as the diastereoisomeric mixture. ^{1}H NMR (60 MHz, $CDCl_3$) δ=2.12 (m, 10H), 5.75 (m, 4H) [lit,[7] 1.2—2.68 (10H), 5.65 (m, 4H)]; ^{13}C NMR (15 MHz, $CDCl_3$) δ=27.41, 27.72 (C4), 32.09, 32.36 (C5), 50.69, 51.04 (C3), 130.96 (C1), 133.78, 133.91 (C2), which support the diastereoisomeric mixture. MS *m/z* (rel intensity) 134 (M^+; 100), 135 (M^++1; 12), 136 (M^++2; 3); IR 3040, 1610 cm^{-1}. GLC analysis of the extract indicated the formation of small quantities of cyclopentenone. Cyclopentanol and cyclopentanone were also detected in the aqueous phase by GLC analysis. The formation of the dimer (1.8 mmol) corresponds only to 14% of the evolved H_2. The recovered ZnS was extracted by THF using Soxhlet, giving oligomeric products (285 mg), which corresponded to 4.2 mmol on basis of cyclopentenyl unit. Mass spectrum of the extract suggested that the oligomers should consist of trimer, tetramer, pentamer, and hexamer.

Photolysis of Cyclohexene and Characterization of Products. The procedure for cyclopentene was followed by using cyclohexene (10 mL. 13-h irradiation) to give comparable results as shown in Table 3. Bi-3-cyclohexen-1-yl (*dl* and *meso*): Bp 105—110 °C/12 Torr (lit,[18] 110/15 Torr), ^{1}H NMR (60 MHz, $CDCl_3$) δ=1.83 (m, 14H), 5.67 (m, 4H), [lit,[18] 1.10—2.33 (m, 14H), 5.40—5.86 (m, 4H)]; ^{13}C NMR (15 MHz, $CDCl_3$) δ=22.30 (C5), 25.42 (C6), 26.03 (C4), 40.2 (C3), 127.63, 127.97 (C1), 130.44, 130.60 (C2), [lit,[18] 22.3, 25.5, 26.1, 40.2, 127.7, 128.0, 130.5, 130.7]; MS *m/z* (rel intensity) 162 (M^+; 100), 163 (M^++1; 15), 164 (M^++2; 4); IR 3030, 1655 cm^{-1}. GLC analysis of the extract indicated the formation of a small quantity of cyclohexenone. IR analysis indicated the presence of the products with hydroxyl or carbonyl groups in the oligomer products (trimer to hexamer).

Photolysis of 2-Methylfuran and Characterization of Products. The procedure for cyclopentene was followed by using 2-methylfuran (10 mL. 8-h irradiation) to give comparable results, as shown in Table 3. The coupling product, 1,2-di(2-furyl)ethane, was produced with a comparable quantity of oligomeric products (trimer to pentamer (by GPC)) and their derivatives with hydroxyl group and/or carbonyl group. 1,2-Di(2-furyl)ethane: Purified by Kugelrohr distillation and chromatography on basic alumina (4.5% water) with petroleum ether; ^{1}H NMR (60 MHz, $CDCl_3$) δ=2.95 (s, 4H), 5.93 (d, 2H), 6.20 (d-d, 2H), 7.23 (m, 2H); ^{13}C NMR (15 MHz, $CDCl_3$) δ=26.72 (CH_2), 105.17 (C3), 110.10 (C4), 140.99 (C5), 154.91 (C2). MS *m/z* (rel intensity) 162 (M^+; 100), 163 (M^++1; 3.3), 164 (M^++3; 0.5); IR 3140, 1605 cm^{-1}. Anal. Found: C, 74.13; H, 6.37%. Calcd for $C_{10}H_{12}O_2$: C, 74.06; H, 6.22%.

Photolysis of Ethylbenzene and Characterization of Products. The procedure for cyclopentene was followed by using ethylbenzene (10 mL. 12-h irradiation) to give the results shown in Table 3. Blackening of the ZnS was observed. The separation and purification were followed by extraction, condensation, chromatography on basic alumina (2.4% water). 2,3-Diphenylbutane crystallized during work-up and the meso type was purified by recrystallization from methanol (mp 124—125 [lit,[19] 124—125]. From the filtrate, the mixture of *meso* and *dl* types was obtained: ^{1}H NMR (60 MHz, $CDCl_3$) δ=0.93 (*meso*), 1.20 (*dl*) (d, 6H), 2.70 (*meso*), 2.80 (*dl*) (m, 2H), 7.13, 7.17 (s, 10H); ^{13}C NMR (15 MHz, $CDCl_3$) as the *meso* and *dl* mixture, *d* 17.97, 20.96 (CH_3),

46.49, 47.27 (CH), 125.68, 126.02, 127.58, 127.76, 128.23, 145.79, 146.44 (C_6H_5); MS *m/z* (rel intensity) 210 (M^+; 100), 211 (M^++1; 19), 212 (M^++2; 2). 2,3-Diphenyl-2-butanol (*threo*, *erythro*): ^{1}H NMR (60 MHz, $CDCl_3$) δ=1.06 (d, CH_3), 1.33 (s, CH_3), 1.63 (br, OH), 3.27 (m, CH), 7.2 (m, C_6H_5). The data were consistent with those reported for the *erythro* and the *threo*;[20] ^{13}C NMR (15 MHz, $CDCl_3$) δ= 15.54, 15.71 (CH_3), 25.93, 29.76 (CH_3), 50.60, 50.99 (CH), 76.13, 76.35 (COH), 125.07, 125.63, 126.28, 126.48, 127.54, 127.63, 127.80, 127.86, 129.19, 142.19, 142.84, 146.83, 147.22 (C_6H_5); MS *m/z* 225 (M^+-1), 218 (M^+-18). 2,3-Diphenyl-2,3-butanediol (*dl*, *meso*): The chromatography separated the *meso* (mp 127—129 [lit,[21] 123—125] and *dl* types and they were assigned by the comparison with the reported data on ^{1}H NMR.[22] ^{1}H NMR (60 MHz, $CDCl_3$) *meso* form: δ=1.48 (s, 6H), 2.54 (s, 2H), 7.13 (s, 10H); *dl* form: δ=1.55 (s, 6H), 2.23 (s, 2H), 7.16 (s, 10H), 2.95 (s, 4H), 5.93 (d, 2H), 6.20 (d-d, 2H), 7.23 (m, 2H); ^{13}C NMR (15 MHz, $CDCl_3$) *meso* form: δ=25.14 (CH_3), 79.1 (COH), 127.2, 127.3, 127.5, 143.7 (C_6H_5); *dl* form: δ=25.37 (CH_3), 78.8 (COH), 127.1, 127.4, 144.0 (C_6H_5); MS *m/z* 241 (M^+-1).

Photolysis of Toluene and Characterization of Products. The procedure for cyclopentene was followed by using toluene (10 mL. 12-h irradiation) to give the results shown in Table 3. Blackening of the catalyst was observed during the reaction. Bibenzyl, dibenzyl sulfide, dibenzyl disulfide were characterized by comparison with authentic samples.

ESR Measurement. The aqueous solution of 2-propanol containing 0.125 mmol of nano-ZnS suspension was prepared in the absence of O_2 under cooling. The solution was placed in a quartz flat cell (1 mm in inner thickness) and radiated with XeCl excimer laser light under the control of temperature. At −90 °C the signal shown in Fig. 9 was observed to increase and to level off in 10 min. The same signal was observed under laser irradiation after the cell was left standing overnight. The photocatalytic H_2 evolution from the solution was observed under 290-nm irradiation at −30 °C.

Semi-Empirical Molecular Orbital Calculations. Molecular orbital calculations by the PM3 method[23] were performed with the MOPAC program (ver. 6.0) using an Iris Indigo R4000 computer. The structural input and output were handled by using the MOL-GRAPH program (ver. 2.8) by Daikin Industries, Ltd.

We thank Dr. T. Sakata (Institute for Molecular Science; currently at Tokyo Institute of Technology) and Dr. K. Hashimoto (Institute for Molecular Science, currently at the Univ. of Tokyo) for helpful discussions, and Dr. Seigo Yamauchi (Kyoto Univ., currently at Tohoku Univ.) for his help in taking the ESR spectra. This work was supported by the Iwatani Naoji Foundation's Research Grant, the Nagase Science and Technology Foundation, and by some Grants-in-aid for Scientific Research Nos. 61550617, 62213021, 03205086, and 04205085 from the Ministry of Education, Science and Culture.

References

1) Part 17: T. Shiragami, S. Fukami, Y. Wada, and S. Yanagida, *J. Phys. Chem.*, **97**, 12882 (1993).

2) S. Yanagida, T. Azuma, Y. Midori, C. Pac, and H. Sakurai, *J. Chem. Soc., Perkin Trans. 2*, **1985**, 1487.

3) S. Yanagida, K. Mizumoto, and C. Pac, *J. Am. Chem. Soc.*, **108**, 647 (1986).

4) S. Yanagida, Y. Ishimaru, Y. Miyake, T. Shiragami, C. Pac, K. Hashimoto, and T. Sakata, *J. Phys. Chem.*, **93**, 2576 (1989).

5) S. Yanagida, M. Yoshiya, T. Shiragami, C. Pac, H. Mori, and H. Fujita, *J. Phys. Chem.*, **94**, 3104 (1990).

6) a) M. Kanemoto, T. Shiragami, C. Pac, and S. Yanagida, *Chem. Lett.*, **1990**, 931; b) M. Kanemoto, T. Shiragami, C. Pac, and S. Yanagida, *J. Phys. Chem.*, **96**, 3521 (1992).

7) a) S. Yanagida, T. Azuma, H. Kawakami, H. Kizumoto, and H. Sakurai, *J. Chem. Soc., Chem. Commun.*, **1984**, 21; b) S. Yanagida, H. Kawakami, K. Hashimoto, T. Sakata, C. Pac, and H. Sakurai, *Chem. Lett.*, **1984**, 1449.

8) S. Yanagida, H. Kizumoto, Y. Ishimaru, C. Pac, and H. Sakurai, *Chem. Lett.*, **1985**, 141.

9) It is worth noting that the powdered nano-ZnS catalyst, which was obtained by drying a freshly prepared nano-ZnS, became effective for the EG formation. This fact can be rationalized by taking into account the surface defects on nano-ZnS formed during work-up as active sites for oxidative quenching sites leading to effective H_2 evolution.[5,7]

10) It should be noted that some crystalline ZnS (cubic, sphalerite) showed a fair activity for the H_2 evolution in the photooxidation of methanol.[7b] The activity may be ascribed partly to the formation of active ZnS particles in the system through dissolution equilibrium, because the solubility product of ZnS (7.4×10^{-27}) is relatively high compared with other insoluble inorganic materials (e.g., CdS; 1.14×10^{-28}).[11]

11) "Solubilities Inorganic and Metal Organic Compounds," ed by W. F. Linkel, D. Van Nostrand Company, Inc., Princeton, New Jersey (1958).

12) D. Griller and F. P. Lossing, *J. Am. Chem. Soc.*, **103**, 1586 (1981).

13) "Encyclopedia of Electrochemistry of the Elements, Organic Sections," ed by J. A. Bard and H. Lund, Marcel Dekker, New York (1978), Vol. 12.

14) "Handbook of Chemistry and Physics," 52nd ed, ed by R. C. Weast, C. R. C. Press, Cleveland (1971), p. E62.

15) a) J. Hawecker, J-M. Lehn, and R. Ziessel, *Nouv. J. Chim.*, **7**, 271 (1983); b) J. Hawecker, J-M. Lehn, and R. Ziessel, *Helv. Chim. Acta.*, **69**, 1990 (1986).

16) a) S. Matsuoka, H. Fujii, T. Yamada, C. Pac, A. Ishida, S. Takamuku, M. Kusaba, N. Nakajima, S. Yanagida, K. Hashimoto, and T. Sakata, *J. Phys. Chem.*, **95**, 5802 (1991); b) S. Matsuoka, T. Kohzuki, Y. Kuwana, A. Nakamura, and S. Yanagida, *J. Chem. Soc., Perkin Trans. 2*, **1992**, 679; c) T. Shiragami, C. Pac, and S. Yanagida, *J. Phys. Chem.*, **94**, 504 (1990).

17) E. E. Van Tamellene, J. I. Brauman, and L. E. Eills, *J. Am. Chem. Soc.*, **93**, 6145 (1971).

18) D. L. J. Clive, P. C. Anderson, N. Moss, and A. Singk, *J. Org. Chem.*, **47**, 1641 (1982).

19) P. Singh, *J. Chem. Soc. C*, **1971**, 714.
20) D. Bellus and K. Schaffner, *Helv. Chim. Acta*, **52**, 1010 (1969).
21) H. D. Becker, *J. Org. Chem.*, **32**, 2140 (1967).
22) M. Lasperas, A. P. Rubalacaba, and M. L. Quiroga-Feijoo, *Tetrahedron*, **36**, 3403 (1980).
23) J. J. P. Stewart, *J. Comput. Chem.*, **10**, 209 (1988).